Towards the development of a biorelevant in vitro method for the prediction of nanoemulsion stability on the ocular surface

Jurišić Dukovski, Bisera; Ljubica, Josip; Kocbek, P; Safundžić Kučuk, Maša; Krtalić, Iva; Hafner, Anita; Pepić, Ivan; Lovrić, Jasmina

Source / Izvornik: **International Journal of Pharmaceutics, 2023, 633**

Journal article, Published version
Rad u časopisu, Objavljena verzija rada (izdavačev PDF)

https://doi.org/10.1016/j.ijpharm.2023.122622

Permanent link / Trajna poveznica: https://urn.nsk.hr/urn:nbn:hr:163:579310

International Journal of Pharmaceutics 633 (2023) 122622

Contents lists available at ScienceDirect

International Journal of Pharmaceutics

journal homepage: www.elsevier.com/locate/ijpharm

Towards the development of a biorelevant *in vitro* method for the prediction of nanoemulsion stability on the ocular surface

Bisera Jurišić Dukovski [a,1], Josip Ljubica [a,1], Petra Kocbek [b], Maša Safundžić Kučuk [c], Iva Krtalić [d], Anita Hafner [a], Ivan Pepić [a], Jasmina Lovrić [a,*]

[a] University of Zagreb Faculty of Pharmacy and Biochemistry, Ante Kovačića 1, 10000 Zagreb, Croatia
[b] University of Ljubljana, Faculty of Pharmacy, Aškerčeva cesta 7, 1000 Ljubljana, Slovenia
[c] Jadran-galenski laboratorij d.d., Svilno 20, 51000 Rijeka, Croatia
[d] R&D, PLIVA Croatia Ltd, TEVA Group Member, Prilaz baruna Filipovića 25, 1000 Zagreb, Croatia

ARTICLE INFO

Keywords:
Eye drops
Nanoemulsion
Chitosan
Dilution
High shear
Dynamic light scattering

ABSTRACT

Ophthalmic oil-in-water nanoemulsions (NEs) are a complex technological platform, representing an advancement in the treatment of dry eye disease. In addition to enabling the incorporation of poorly soluble active pharmaceutical ingredients (APIs), NEs provide prolonged residence time of APIs and other formulation components and consequent replenishment and stabilization of the compromised tear film. Ophthalmic NEs have been on the market for over 20 years, but considering their complexity, as well as the complex nature of the ocular surface, they are still a poorly understood advanced dosage form. The objective of this study was to develop a biorelevant *in vitro* method that would be able to predict the behavior of ophthalmic NEs after application. With that goal, NE formulations differing in critical material attributes and critical formulation variables were employed and subjected to simulated tear turnover and blinking. By gradually increasing the complexity of the *in vitro* method, we were able to detect key parameters influencing NE stability. The undertaken study presents a step forward in the development of *in vitro* tools that are fundamental to the reliable, cost and time-effective development of innovative and generic topical ophthalmic NEs.

1. Introduction

Oil-in-water nanoemulsions (NEs) represent an advancement in dry eye disease (DED) treatment. They serve as a technological platform for the incorporation of poorly water-soluble anti-inflammatory active pharmaceutical ingredients (APIs), enabling prolonged residence time of APIs and other formulation components at the ocular surface and consequently providing anti-inflammatory effects, replenishment, and stabilization of the compromised tear film (TF) (Daull et al., 2020; Singh et al., 2020).

NEs are complex drug products consisting of oil nanodroplets dispersed in water and stabilized by surfactants. They may also contain micelles due to the presence of surfactant molecules in excess (Bellantone et al., 2022; Petrochenko et al., 2018). Their site of action is restricted primarily to the ocular surface, and hence, the clinical performance of NEs depends on the interplay between the formulation physicochemical properties and physiological environment of the complex nature of the ocular surface (Daull et al., 2020). The goal of NE-based drug product development is to achieve an optimal balance between the formulation properties (droplet size and size distribution, zeta potential, formulation osmolality, surface tension and stability) and the formulation effect on the ocular surface (lipid and lubricant supplementation, prolonged residence time, drug permeation in corneal and conjunctival epithelium, anti-inflammatory effect) (Walenga et al., 2019; Xu et al., 2015). Owing to its unique anatomical and physiological functions, a complex ocular surface presents a special challenge for both

Abbreviations: API, active pharmaceutical ingredient; ATS, artificial tear solution; CsA, cyclosporine A; DD, degree of deacetylation; DDW, double-distilled water; DED, dry eye disease; DLS, dynamic light scattering; ELS, electrophoretic light scattering; EMA, European Medicines Agency; FDA, Food and Drug Administration; LD, laser diffraction; LM_w, low molecular weight; NE, nanoemulsion; OLIGO, oligosaccharide lactate; PDI, polydispersity index, RI, refractive index; RT, room temperature; TF, tear film; TFLL, tear film lipid layer.

* Corresponding author.
E-mail address: jasmina.lovric@pharma.unizg.hr (J. Lovrić).

[1] These authors contributed equally to this work.

https://doi.org/10.1016/j.ijpharm.2023.122622
Received 14 October 2022; Received in revised form 13 January 2023; Accepted 14 January 2023
Available online 18 January 2023

the design and performance evaluation of NEs (Xu et al., 2015).

According to the current understanding, mixing of an NE with a hyperosmolar TF primarily leads to TF dilution and a decrease in its osmolality (Daull et al., 2020). This effect lasts for a couple of minutes and is related to the fast turnover of the aqueous phase of the tears. The interaction of a NE with TF components, continuous dilution with the tear aqueous phase and blinking-related shear stress eventually compromises the physical stability of oil nanodroplets. The oil phase shows sustained residence time at the ocular surface (3 to 4 h after instillation (Maïssa et al., 2010; Stevenson et al., 2000; Walenga et al., 2019). Nonpolar lipids from oil nanodroplets merge with the tear film lipid layer (TFLL) and increase its thickness (Daull et al., 2020). Polar lipids stabilize the interface between the TFLL and the aqueous phase of the TF. Other hydrophilic surfactants from the NE formulation can be adsorbed at the TFLL interface and slightly penetrate into the lipid film, synergistically contributing to TFLL stabilization, even though they are eventually squeezed out of the TFLL interface after repeated cycles of eye blinking. Positively charged surfactants/polymers can also have an important role in the stabilization of the TFLL and its interface. At the interface of the TFLL, they are oriented toward the aqueous phase with a positively charged head. Through electrostatic interactions with the positively charged moieties exposed to water, the negatively charged soluble proteins (mucins, lysozyme) present in the aqueous phase of the TF are adsorbed at the interface of the TFLL. Adsorbed proteins may help to reduce the surface tension of the TFLL and thus further improve the overall stability of the TF. It is thought that all these events together lead to replenishment and stabilization of the compromised TF.

Restasis® (cyclosporine A (CsA) ophthalmic emulsion, 0.05 %, Allergan) was the first commercial ophthalmic NE approved by the Food and Drug Administration (FDA) in 2002. Cationorm®, a cationic API-free NE (Santen, Novagali Pharma), was marketed as a medical device in 2008, providing long-lasting relief from the uncomfortable symptoms of DED, while Ikervis®, a cationic NE containing CsA (1 mg mL^{-1}), was approved by the European Medicines Agency (EMA) in 2015 for severe keratitis in adult patients with DED. In 2022, the FDA approved the first generic of Restasis® (Mylan, Viatris).

Ophthalmic NEs have been on the market for over 20 years, but considering their complexity, as well as the complex nature of the ocular surface, they are still a poorly understood advanced dosage form. To deepen the knowledge on NEs and to improve their development, there is an increasing need to evaluate NE physical stability under ocular conditions, comprising tear turnover and blinking. If reference and generic NE show similar robustness to dilution and simulated blinking *in vitro*, it is expected that they will show comparable physical stability profiles on the eye surface, which is a prerequisite for their comparable efficacy and safety. However, to date, there are no data reported on NE behavior upon dilution *in vivo*. In this study, for the first time, the focus is placed on the development of a biorelevant *in vitro* method for the prediction of NE stability upon instillation on the eye surface. For that purpose, NE formulations differing in critical material attributes and critical formulation variables were subjected to continuous dilution by artificial tear solutions and blinking-related shear force. Consequently, NE resistance to the investigated stress conditions was assessed. The undertaken study presents a step forward in the development of *in vitro* tools fundamental to the successful development of topical ophthalmic NEs.

2. Materials and methods

2.1. Materials

For preparation of NEs, the following substances were used: Miglyol® 812 (Fagron, Rotterdam, Netherlands), lecithin (Lipoid S 45, Lipoid, Ludwigshafen, Germany), Kolliphor® EL (BASF, Ludwigshafen, Germany), glycerol (Fagron), low molecular weight (LM_w) chitosan (M_w range 50–190 kDa, degree of deacetylation (DD) range 75–85 %; Sigma-Aldrich, Steinheim, Germany), and chitosan oligosaccharide lactate (M_w range 4–6 kDa, DD greater than 90 %; Sigma-Aldrich). Artificial tear solution (ATS 0) was prepared by dissolving sodium citrate dihydrate (0.441 mg mL^{-1}, T.T.T. ltd., Croatia), $Na_2HPO_4{\cdot}2H_2O$ (4.272 mg mL^{-1}, Fluka Chemie GmbH, Switzerland), $KHCO_3$ (0.3 mg mL^{-1}, VWR International, USA), NaCl (5.26 mg mL^{-1}, Gram-mol, ltd., Zagreb, Croatia), KCl (1.193 mg mL^{-1}, Gram-mol ltd.), $CaCl_2$ (0.0555 mg mL^{-1}, Gram-mol ltd.), Na_2CO_3 (1.272 mg mL^{-1}, Gram-mol ltd.), HCl (2.6 mg mL^{-1}, Carlo Erba Reagents GmbH, Emmendingen, Germany), D-glucose monohydrate (0.036 mg mL^{-1}, Gram-mol ltd.) and urea (0.072 mg mL^{-1}, Gram-mol ltd.) in double-distilled water (DDW). For preparation of ATS with lipids (ATS 1a), the following lipids were used: triolein (0.015 mg mL^{-1}), phosphatidyl choline (0.0005 mg mL^{-1}), cholesterol (0.0018 mg mL^{-1}), oleic acid (0.0018 mg mL^{-1}), methyl oleate (0.012 mg mL^{-1}) and cholesteryl oleate (0.024 mg mL^{-1}), all purchased from Sigma-Aldrich. For preparation of ATS with mucin (ATS 1b), bovine submaxillary mucin (0.15 mg mL^{-1}, Sigma-Aldrich) was used. ATS 2 was prepared by mixing all the salts, glucose, urea, lipids and mucin. For preparation of the most complex ATS (ATS 3), the following proteins were used: bovine albumin (0.2 mg mL^{-1}), hen egg lysozyme (1.9 mg mL^{-1}), bovine submaxillary mucin (0.15 mg mL^{-1}), bovine colostrum lactoferrin (1.8 mg mL^{-1}) and bovine immunoglobulin G (0.02 mg mL^{-1}), all purchased from Sigma-Aldrich. The commercially available ophthalmic NE Cationorm® (Santen, France) was obtained from the pharmaceutical wholesaler.

2.2. Methods

2.2.1. Preparation of artificial tear solution

Artificial tear solutions with different levels of complexity (ATS 0 – ATS 3) were prepared as previously reported (Lorentz et al., 2011). ATS 0 was prepared by dissolving all the salts, glucose and urea in DDW. The dissolution was accelerated by ultrasonication in a water bath for 2 min. The obtained solution was filtered through a regenerated cellulose membrane filter (pore size 0.2 μm, Sartorius, Göttingen, Germany). The pH of ATS 0 was 6.70, and the osmolality was 305 mOsm kg^{-1}. For preparation of ATS 1a, the concentrated lipid stock solution was prepared first. The lipids were warmed to room temperature (RT) and dissolved in a mixture of hexane ether (1:1, *V/V*) at concentrations of 32, 3.6, 3.6, 24, 48 and 1 mg mL^{-1} for triolein, cholesterol, oleic acid, oleic acid methyl ester, cholesteryl oleate and phosphatidyl choline, respectively. To prepare ATS 1a, 0.5 mL of the lipid stock solution was added to 1 L of ATS 0, followed by a 30-min ultrasonication. The pH and osmolality of ATS 1a were 6.62 and 325 mOsm kg^{-1}, respectively. ATS 1b was prepared by the addition of bovine submaxillary mucin to ATS 0, followed by ultrasonication at 37 °C for no more than 5 min to prevent mucin destruction. The pH and osmolality of ATS 1b were 6.61 and 319 mOsm kg^{-1}, respectively. ATS 2, which contained salts, glucose, urea, lipids, and mucin, was prepared by adding mucin to ATS 1a. The pH and osmolality of ATS 2 were 6.66 and 321 mOsm kg^{-1}, respectively. ATS 3 was prepared by adding all the proteins to ATS 2 and a subsequent 5-min sonication at 37 °C. The pH and osmolality of ATS 3 were 6.71 and 325 mOsm kg^{-1}, respectively. The pH values of ATS 0-ATS 3 were within the pH range of a normal, healthy TF (6.5–7.6) (Abelson et al., 1981) and were therefore not additionally adjusted.

2.2.2. Preparation of ophthalmic nanoemulsions

NEs were prepared in triplicate using a microfluidizer (Model LM20, Microfluidics®, USA), as previously described (Jurišić Dukovski et al., 2020). The first step was preparation of the oil phase by dissolving lecithin in Miglyol® 812 (1:50, *w/w*) at RT under magnetic stirring. In the case of NEs with chitosan, LM_w chitosan was first dissolved in 0.5 % (*w/w*) acetic acid at RT under magnetic stirring. The solution was then filtered and added to the aqueous solution of Kolliphor® EL and glycerol (NE water phase), while chitosan oligosaccharide lactate (OLIGO) was directly dissolved in the water phase. NEs without chitosan or

Kolliphor® EL were prepared according to the same preparation procedure without the addition of the mentioned components. The oil phase was added to the aqueous phase at RT under magnetic stirring, and the obtained dispersion was further prehomogenized with Ultra-Turrax® (IKA-Werke GmbH & Company, Germany) for 5 min at 15000 rpm. The obtained coarse emulsion was then processed on the microfluidizer under a pressure of 1000 bar for 5 cycles. The NE composition is shown in Fig. 1.

2.2.3. Physicochemical characterization of ophthalmic nanoemulsions

Viscosity, osmolality and pH

The viscosity of the NEs was determined at a shear rate from 20 to 100 s^{-1} at 25 °C using an Anton Paar MCR102 rheometer (Graz, Austria) equipped with a cone-plate measuring system (CP 50–1, cone angle 1°, trim position 102 μm). The osmolality of the NEs was determined by the freezing point depression method using an OsmoTECH Osmometer (Advanced Instruments, Norwood, MA, USA). The pH of the NEs was determined by direct measurement using a Seven Multi pH/conductometer (Mettler Toledo, Columbus, OH, USA) at RT. All measurements were performed in triplicate.

2.2.4. Determination of droplet size and size distribution in diluted nanoemulsions using dynamic light scattering

The droplet size and polydispersity index (PDI) of the NEs were determined at 25 °C by dynamic light scattering (DLS) using a Zetasizer Ultra (Malvern Panalytical ltd, Malvern, UK). Each NE formulation was diluted (10–1000 times, *V/V*) and filtered through a polyethersulfone membrane filter (0.45 μm pore size, Macherey-Nagel, Düren, Germany) DDW, glycerol aqueous solution (2.5 %, *w/w*) or ATS 0, and it was placed in a standard disposable cuvette (DTS0012) for measurement. The material refractive index (RI) was set to that of Miglyol® 812 (1.45), and its absorption was set to 0.01. Dispersant viscosity was determined at a shear rate from 20 to 100 s^{-1} at 25 °C using an Anton Paar MCR102 rheometer equipped with a cone-plate measuring system (CP 50–1, cone angle 1°, trim position 102 μm). Dispersant RI was measured using an Abbe laboratory refractometer (Carl Zeiss, Oberkochen, Germany). The viscosity and RI for water, 2.5 % glycerol and ATS 0 were set to 0.8900 mPa·s and 1.330, 0.9916 mPa·s and 1.330, and 0.8261 mPa·s and 1.3345, respectively. Measurements were performed in triplicate at 25 °C with a 60-s equilibration time. Attenuation of the laser was determined automatically by the device to maintain the optimal count rate of scattered light. The angle of detection was set to 174.7°.

2.2.5. Determination of droplet size distribution in diluted nanoemulsions using laser diffraction

The droplet size distribution was determined by laser diffraction (LD) using a Mastersizer 3000 (Malvern Pananalytical ltd. equipped with a Hydro SV sample cell with a magnetic stirrer. DDW, 2.5 % glycerol or ATS 0 were used to determine the background signal. After background measurement, NE formulation was added to the measuring cell to achieve dilutions of 1:50, 1:100 or 1:300 (*V/V*). Obscuration was kept between 1 and 20 % throughout all the measurements. The diluted NEs were equilibrated for 10 s before measurement. Each measurement was performed in triplicate. The results are expressed as volume diameters D_v10, D_v50 and D_v90.

2.2.6. Zeta potential analysis

The zeta potential of NE droplets was determined at 25 °C by electrophoretic light scattering (ELS) using a Zetasizer Ultra. NE samples were diluted (10–1000 times, *V/V*) with filtered (0.45 μm pore size) glycerol aqueous solution (2.5 or 1.6 %, *w/w*) or ATS 0 and placed in a disposable folded capillary cell (DTS1070) for measurement. The dispersant viscosity and RI were set to the values of 2.5 % glycerol or ATS 0. The values measured for 1.6 % glycerol (0.9362 mPa·s and RI 1.330) were used to determine the zeta potential of droplets in Cationorm®. Measurements were performed in triplicate at 25 °C with a 60-s

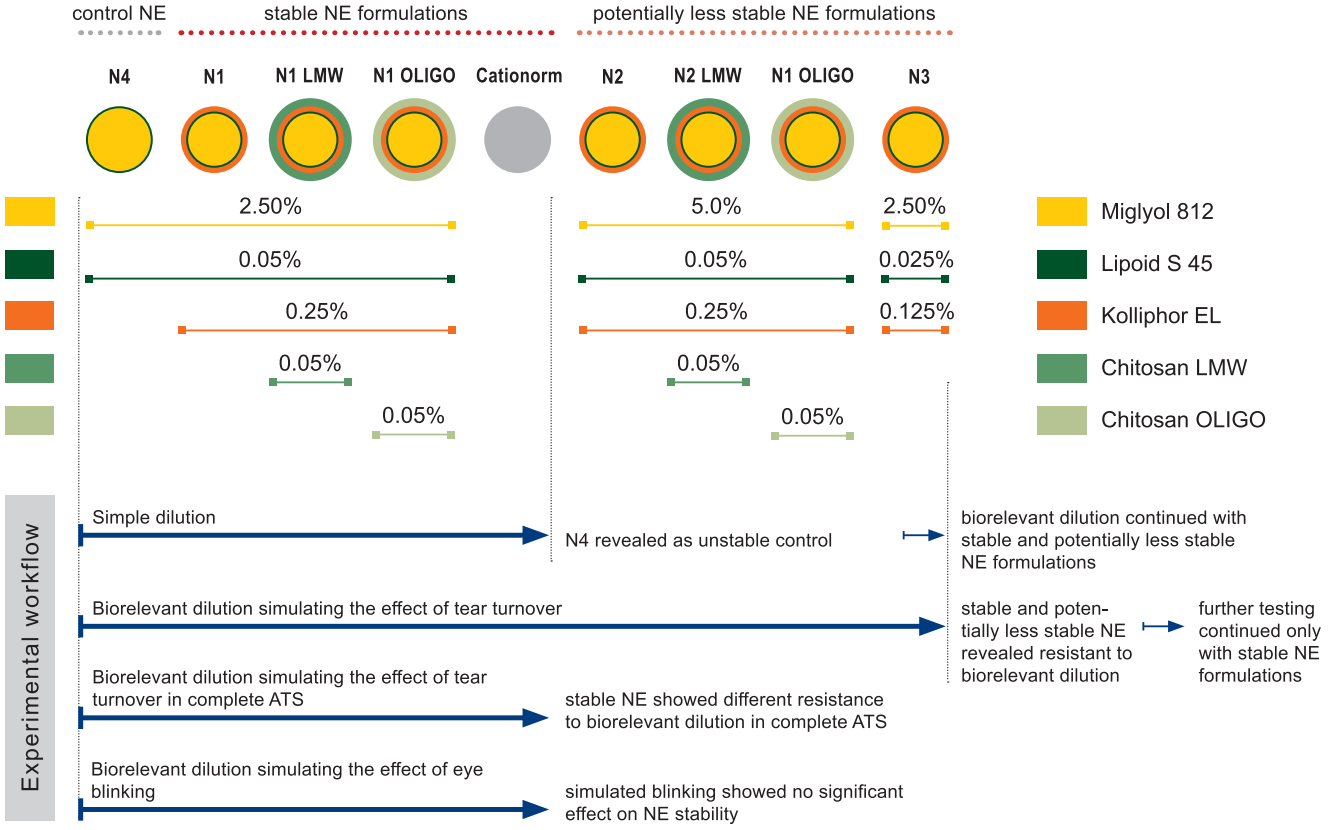

Fig. 1. Schematic representation of the experimental workflow.

equilibration time. Attenuation of the laser and voltage selection were set automatically.

2.2.7. Analysis of nanoemulsion stability under simulated tear turnover

To investigate the effect of tear turnover on NE physical stability, NEs were mixed with ATS 0, 1a, 1b, 2 or 3 in a beaker at a 25:7 (*V/V*) ratio. The sample was placed on an orbital shaker (50 rpm) and thermostated at 34 °C, and the dilution experiment was performed for 40 min. Each minute, 16 % of the sample volume was removed with a pipette and replaced with the same amount of fresh ATS (warmed to 34 °C) to simulate TF turnover *in vivo*. At predetermined time points, NE droplet size and PDI were measured using a Zetasizer Ultra. The measurement parameters were set as described in the section *Determination of droplet size and size distribution in diluted nanoemulsions using dynamic light scattering*, and only the equilibration time was set to 0 s.

2.2.8. Analysis of nanoemulsion stability under simulated eye blinking

To investigate the effect of eye blinking on NE physical stability, the NEs were first diluted 5 times (*V/V*) with ATS 2, which simulates the natural dilution of an NE on the ocular surface that occurs approximately 9 min after NE application. The NEs were then subjected to a high shear rate of 5000 s^{-1} for 1 s (which simulates 1 blink), immediately followed by a nondestructive oscillatory measurement at a frequency of 1 Hz and an amplitude of 1 % for 1 min (which simulates the time period between 2 consecutive blinks) (Destruel et al., 2020). The cycle was repeated 10 times in a row to simulate a period of 10 blinks, and it was performed at 34 °C using an Anton Paar MCR102 rheometer equipped with a cone-plate measuring system (CP 50–1, cone angle 1°, trim position 102 μm). After that, the droplet size and PDI of diluted NEs were determined. An NE sample (approximately 100 μL) was collected with a pipette and placed in an ultralow volume cuvette (ZEN2112, Malvern Panalytical ltd.) for size and PDI measurement by DLS, as described in the section 2.2.4. *Determination of droplet size and size distribution in diluted nanoemulsions using dynamic light scattering.*

3. Results and discussion

3.1. Physicochemical characterizations of ophthalmic nanoemulsions

The objective of this study was to investigate the fate of ophthalmic NEs differing in critical material attributes and critical formulation variables upon their instillation by *in vitro* simulation of the effect of tear turnover and blinking. Miglyol®-based oil-in-water NEs stabilized by lecithin (Lipoid S 45), Kolliphor® EL and chitosan (LM_W or OLIGO) without an API were selected as model formulations (Fig. 1). The mucoadhesive biopolymer chitosan was chosen to provide prolonged retention of the NE formulation on the ocular surface. Two types of chitosan were used, namely, LM_w chitosan (50–190 kDa) and chitosan OLIGO (4–6 kDa), to examine the effect of chitosan molecular weight on the NE physical stability under simulated *in vivo* conditions. Fat-free soybean lecithin (Lipoid S 45) with 45 % (*w/w*) phosphatidylcholine and 10–18 % (*w/w*) phosphatidylethanolamine, two constituents of the natural TF (Dean & Glasgow, 2012; Jones et al., 2017; Saville et al., 2011), was selected as an anionic surfactant enabling interaction with chitosan. Kolliphor® EL, a nonionic surfactant commonly used in ophthalmic products, was chosen as the second (more hydrophilic) surfactant to optimize the droplet size and stability of the formulations.

The NE formulations N1 and N1 LMW were developed previously by our research group for symptomatic treatment of mild-to-moderate DED (Jurišić Dukovski et al., 2020). The formulations were characterized as physically stable at 2–8 °C and 15–25 °C for at least 30 days, and their stability was also confirmed with several stress tests (heating–cooling cycles, centrifugation and freeze–thaw cycles), which had almost no effect on the NE droplet size, PDI or droplet zeta potential. For the purpose of this study, formulation N1 OLIGO was prepared following the same procedure used for N1 LMW, which utilized chitosan OLIGO instead of LM_w chitosan. The formulation N4 containing Miglyol® 812 and lecithin in the dispersed phase was prepared as a control without additional stabilizers.

A commercially available ophthalmic NE Cationorm® was introduced to the study as a marketed reference formulation. Cationorm® is composed of 1 % (*w/w*) mineral oil (light and heavy) and 0.002 % (*w/w*) cetalkonium chloride forming the oil phase and 0.3 % (*w/w*) tyloxapol, 0.1 % (*w/w*) poloxamer 188, 1.6 % (*w/w*) glycerol, 0.071/0.006 % (*w/w*) tris-HCl/trometamine (buffer) and water for injection up to 100 % (*w/w*) forming the aqueous NE phase (Georgiev et al., 2017).

3.2. Impact of simple dilution on nanoemulsion droplet size, size distribution and zeta potential

Dispersion of the oil droplets in the water phase resulting in a stable nonequilibrium NE is achieved by kinetic energy input (i.e., high shear force). Surfactants present in NE formulations reduce interfacial tension and slow the process of interfacial area reduction, thereby creating a kinetically stable system (Petrochenko et al., 2018; Tadros et al., 2004). Due to kinetic stabilization, droplets in an NE are expected to be stable upon dilution; thus, their size and size distribution will not change significantly upon dilution. The droplet size distribution is most commonly determined by DLS, which usually requires dilution of the sample prior to measurement. Thus, the literature reports DLS measurements of NEs diluted 100–1000 times, usually with purified water (Isailović et al., 2016; Khatri & Shao, 2017; Krämer et al., 2019; Kumar & Mandal, 2018; Lefebvre et al., 2017; Savić et al., 2019).

A recent study reported an in-depth assessment of the droplet size and size distribution of polydisperse CsA-loaded NEs using five fundamentally different techniques, namely, DLS, LD, nanoparticle tracking analysis, cryogenic transmission electron microscopy and 2-dimensional diffusion ordered spectroscopy nuclear magnetic resonance (Petrochenko et al., 2018). The droplet size of CsA NEs measured using different techniques indicated that dilution of NE with ultrapure water does not give rise to a detectable change in the NE droplet size. The overestimation of droplet size in DLS size measurements for CsA NEs at high concentrations (e.g., stock formulation or less diluted NE samples) was primarily attributed to interferences of the excipients (carbomer copolymer type A, Carbopol® polymer 1342 and hydroxypropyl methyl cellulose K15 M, three types of viscosity enhancing polymers) on measured droplet size. The authors speculate that excipients with different chemistries may interact differently with NE droplets, resulting in variations in measured droplet sizes, which might be overcome by either testing NEs under diluted conditions or by using a technique less susceptible to these interferences. However, in that study, NEs were diluted with ultrapure water only. To predict NE *in vivo* performance, knowledge about NE behavior upon dilution with biorelevant medium is crucial.

In this study, stable NEs and respective controls were first subjected to simple dilution with DDW, 2.5 % glycerol or ATS 0 (Fig. 1). The droplet size measurement was carried out on a series of diluted ophthalmic NEs by DLS. The NEs were diluted with DDW, the most commonly used dilution medium in DLS measurements, 2.5 % glycerol, the external phase of the prepared NEs, or a biorelevant dilution medium, namely, an artificial tear solution containing salts, glucose and urea in DDW (ATS 0). Undiluted NE formulations were not measured because, according to the manufacturer's instructions, they were too concentrated to give reliable results. The DLS technique is based on the Brownian motion of droplets. This method measures the rate at which the intensity of the scattered light fluctuates due to droplet movement. Small droplets move faster than large droplets, causing the scattered light intensity to fluctuate more rapidly. In the case of viscous NE formulations showing shear-thinning behavior, dilution significantly reduces sample viscosity and thus affects the measured droplet size, according to the Stokes-Einstein equation. However, this was not the case in this study, since all the NEs were characterized by very low

viscosity values (Table 1), similar to the viscosities of the pure dilution media. They behaved as Newtonian fluids when subjected to a gradually increasing shear rate. At very high NE concentrations, droplet–droplet interactions hinder Brownian motion, causing slower droplet movement and falsely larger average droplet size results (Petrochenko et al., 2018). Thus, an appropriate dilution of NE is crucial to obtain accurate measurement results. In Fig. 2, the average droplet size (hydrodynamic diameter) and polydispersity index (PDI) of a series of diluted NE formulations are shown. The average droplet size of NE formulations N1, N1 LMW, N1 OLIGO and Cationorm® was below 200 nm, irrespective of the dilution factor or dilution media used. The PDI of NE formulations N1, N1 LMW and N1 OLIGO slightly decreased with dilution. This decrease can be ascribed to the multiple scattering effect at higher droplet concentrations, where the photons scattered from one droplet are rescattered from the neighboring droplets before reaching the detector. When multiply scattered light is interpreted as single scattering, it leads to faster fluctuations, smaller apparent average droplet size and an increase in apparent polydispersity of the sample (Ragheb & Nobbmann, 2020). In the case of NE formulations N1, N1 LMW and N1 OLIGO, droplet–droplet interactions that hindered Brownian motion probably cancelled the multiple scattering effect at lower NE dilutions, resulting in constant droplet size but higher PDI. On the other hand, the PDI of Cationorm® seems to be less influenced by dilution, probably due to lower oil phase content (1 %), compared to our NE formulations (2.5 %), and similar droplet size as in NE formulations N1, N1 LMW and N1 OLIGO, giving rise to lower droplet concentration, less droplet–droplet interactions and multiple scattering effects. The NE formulation N4 prepared with lecithin as the only surfactant showed higher but constant average droplet size and PDI values throughout the dilutions in DDW and 2.5 % glycerol. However, when ATS 0 was used as a dilution medium, an instant droplet size increase (from approximately 270–300 nm to 430–560 nm) was observed. The PDI also increased but was still close to 0.2. The tendency for droplet coalescence and growth to occur at high ionic strengths can be attributed to electrostatic screening effects, i.e., accumulation of counterions around the nanodroplet surface reducing electrostatic repulsion (Israelachvili, 2011; McClements, 2015; Ozturk et al., 2014; Sandoval-Cuellar et al., 2020). Thus, the addition of the second, more hydrophilic surfactant Kolliphor® EL was crucial to assure NE resistance to destabilization due to dilution with biorelevant medium.

DLS is one of the most commonly used techniques for the determination of droplet size and size distribution in NEs. However, the DLS results encompass only the average droplet size and PDI (intensity-weighted distribution) of the droplets in an NE. Thus, to confirm that the NE formulations N1, N1 LMW, N1 OLIGO and Cationorm® resist destabilization upon dilution with different media, LD was employed as an additional viable and commonly used technique for NE characterization, providing volume-weighted droplet size distribution as the measurement result. LD measurements were performed using a Mastersizer 3000 on the NEs diluted 50, 100 and 300 times with DDW, 2.5 % glycerol, or ATS 0 (Fig. 3). Dilution factors of 10 and 1000 times were omitted in LD measurements due to the obscuration levels of the detector being too high or too low. The impact of dilution on droplet size in DDW and 2.5 % glycerol was minimal for all the NEs, and these dilution effects were consistent with the results obtained using DLS. However, when ATS 0 was used as the dilution medium, a significant droplet size increase (D_v10, D_v50 and D_v90 from 104.8 ± 0.4 nm, 144.4 ± 0.5 nm, and 581.0 ± 59.7 nm in 2.5 % glycerol, respectively, to 236.6 ± 13.3 nm, 431.2 ± 30.3 nm, and 735.8 ± 57.9 nm in ATS 0, respectively) was observed in the case of N1 LMW, an effect that was not detected by DLS.

The droplet size distribution by LD was also determined for formulation N4, but only with a dilution factor of 300. Dilution of formulation N4 50 and 100 times led to overrun of the appropriate level of obscuration, which made the measurement result unreliable. The obtained volume droplet distributions (D_v10, D_v50 and D_v90) for NE formulation N4 diluted in DDW were 139.3 ± 24.6 nm, 246.8 ± 30.2 nm, and 409.2 ± 28.7 nm, respectively. In 2,5% glycerol, D_v10, D_v50 and D_v90 were 133.0 ± 15.4 nm, 243.6 ± 18.5 nm, 405.8 ± 21.5 nm, while in ATS 0, higher values were obtained: 143.3 ± 7.0 nm, 284.0 ± 14.3 nm and 524.2 ± 54.4 nm. That said, LD confirmed the results of DLS measurement, which indicates that the NE formulation N4 had a larger average droplet size and that dilution with ATS 0 resulted in a droplet size increase.

Zeta potential is the key parameter that affects NE stability due to the electrostatic repulsion between droplets carrying positive or negative surface charges (Kaszuba et al., 2010). Zeta potential also affects NE performance upon instillation on the eye surface. Positively charged (i.e., cationic) NEs exert prolonged residence time on the ocular surface due to a reduction in the contact angle, increased spreading coefficient and wettability of the droplets, which is caused by electrostatic interactions with the negatively charged surface of the cornea (Gan et al., 2013). Thus, it is also important to know how dilution with different media affects the NE zeta potential. In an attempt to study the effects of different media, the NEs in this study were diluted 10–1000 times with the NE water phase (2.5 % glycerol or 1.6 % glycerol in the case of Cationorm®) to keep the nanodroplet environment unchanged and with ATS 0, a more biorelevant medium that mimics the conditions in terms of ionic composition to which the NEs are exposed after instillation to the eye. The zeta potential measurement results of the NEs diluted with the NE water phase are shown in Fig. 4a. NE formulations N1 and N4 show a negative zeta potential (-30 – -46 mV) that persists throughout all dilutions. The NE formulations N1 LMW and N1 OLIGO coated with positively charged chitosan molecules were characterized by a highly positive zeta potential, which decreased as the dilution factor increased (from 64 to 27 mV and from 63 to 23 mV for N1 LMW and N1 OLIGO, respectively). This could be a consequence of chitosan desorption from the droplet surface at higher dilutions. Cationorm®, on the other hand, is characterized by a slightly positive zeta potential (7–9 mV) that turns to a slightly negative one (-14 mV) at dilutions greater than 100 times. It seems that despite its high lipophilic character (Lallemand et al., 2012), positively charged cetalkonium chloride leaves the nanodroplet surface at higher dilutions. Significantly lower absolute zeta potential values were obtained when the NEs were diluted with ATS 0 (Fig. 4b). The thickness of the electrical double layer surrounding an NE droplet depends upon the concentration of ions in the dilution medium. According to DLVO theory, the higher the ionic strength is, the more compressed the double layer becomes, leading to a decrease in the absolute zeta potential value. The zeta potential values obtained after dilution in ATS 0 were probably the consequence of the electrical double layer compression and, in the case of the NEs N1 LMW, N1 OLIGO and Cationorm®, chitosan or cetalkonium chloride desorption from the nanodroplet surface. According to these findings, it is not clear whether the benefits of the application of cationic NEs to the eye are a consequence of their positive zeta potential. However, this is a topic that deserves careful and more extensive research and as such is beyond the scope of this study.

In summary, the droplet size measurements using DLS and LD techniques suggest that simple NE dilution with water or NE water phase does not result in detectable droplet size changes. Moreover, adequately stabilized NEs showed resistance to simple dilution with the biorelevant

Table 1
Nanoemulsion physicochemical properties.

Formulation	Viscosity (mPa·s)	Osmolality (mOsm kg^{-1})	pH
N1	1.06 ± 0.02	297.0 ± 1.4	6.30 ± 0.49
N1 LMW	1.79 ± 0.01	301.5 ± 2.1	4.62 ± 0.01
N1 OLIGO	1.80 ± 0.02	300.5 ± 2.1	4.31 ± 0.06
N2	1.15 ± 0.02	287.5 ± 3.5	6.63 ± 0.16
N2 LMW	2.15 ± 0.05	302.5 ± 0.7	4.67 ± 0.10
N2 OLIGO	2.06 ± 0.11	303.0 ± 2.8	4.40 ± 0.13
N3	1.06 ± 0.01	297.0 ± 2.8	5.96 ± 0.05
N4	1.05 ± 0.01	294.0 ± 5.7	5.54 ± 0.03

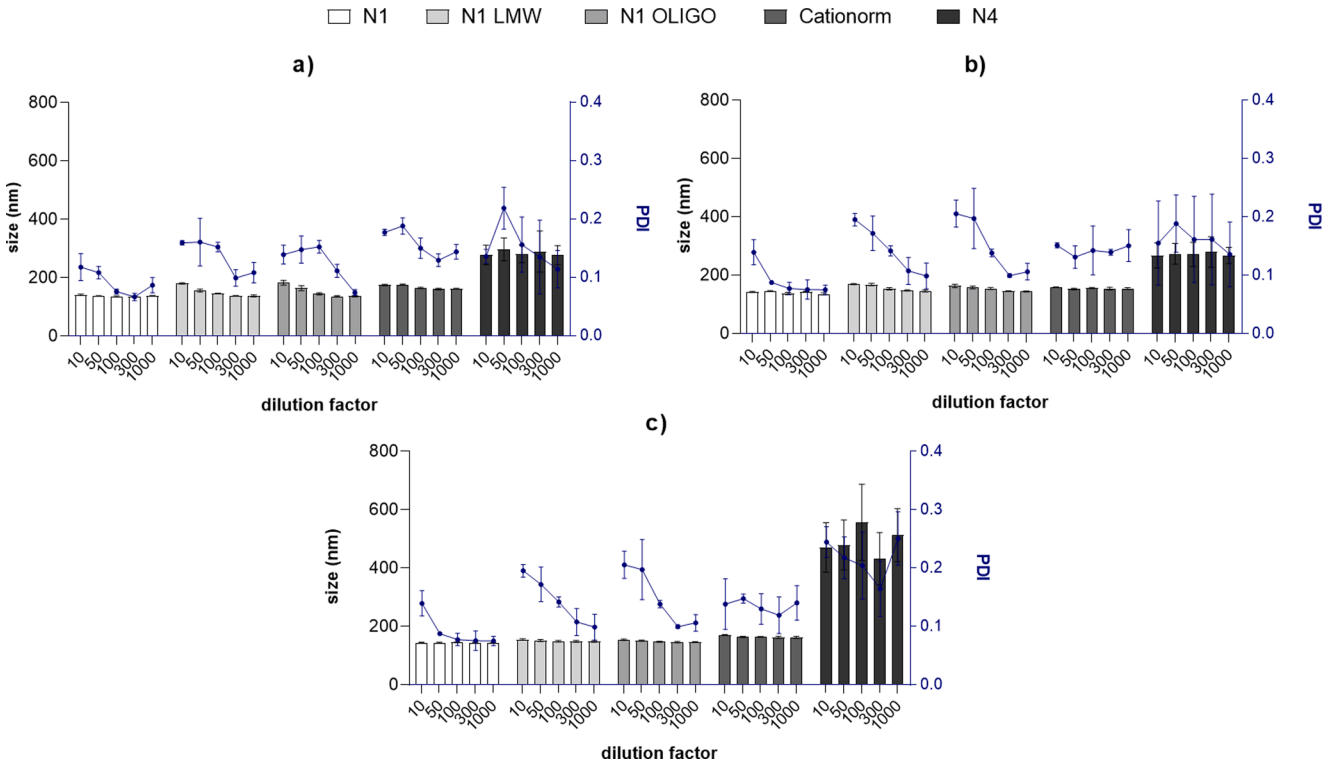

Fig. 2. Average hydrodynamic droplet size (bars) and polydispersity index (PDI, circles) of a series of DDW (a), 2.5 % glycerol (b), and ATS 0 (c)-diluted NEs. Data are expressed as the mean ± SD (n = 3).

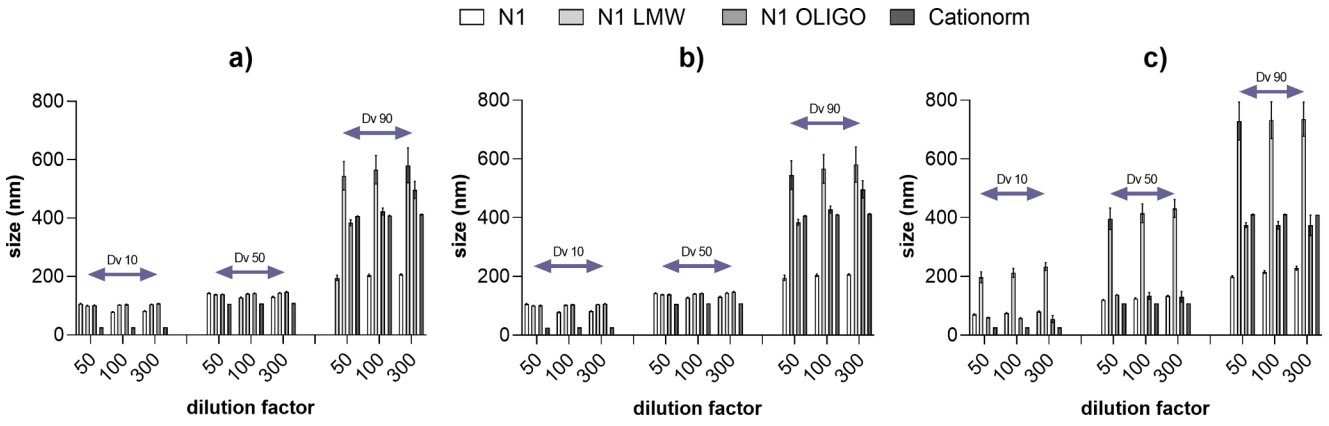

Fig. 3. Droplet size distribution (D_v10, D_v50 and D_v90) determined by LD of a series of DDW (a), 2.5 % glycerol (b), and ATS 0 (c)-diluted NEs. Data are expressed as the mean ± SD (n = 3).

dilution medium ATS 0. The increase in droplet size upon dilution with ATS 0, demonstrated by DLS and LD, was observed only for the formulation stabilized with only one stabilizer.

3.3. Nanoemulsion stability under simulated tear turnover

To perform a comprehensive investigation, we prepared additional NE formulations (Fig. 1). A series of potentially less stable NE formulations was prepared, namely, NEs with double the amount of the oil phase, with the same chitosan and/or surfactant content (formulations N2, N2 LMW and N2 OLIGO), and a NE with the same oil content but with half the amount of the stabilizers (lecithin and Kolliphor® EL) (formulation N3). It is important to emphasize that the potentially less stable NEs were visually unchanged throughout 3 months of storage at 2–8 °C.

Upon instillation on the eye surface or conjunctival sac, NEs are immediately mixed with tear fluid composed of a wide variety of salts, lipids, mucins and proteins (Willcox et al., 2017). In this study, the NEs were mixed with ATS of different levels of complexity (Levels 0–3) according to the components present in the ATS. Level 0 represented ATS containing only salts, glucose and urea. Level 1a, in addition to salts, urea and glucose, contained lipids naturally present in the TF (triolein, cholesterol, oleic acid, oleic acid methyl ester, cholesteryl oleate and phosphatidylcholine), while level 1b contained mucin instead of lipids. Level 2 biorelevant media represented complex ATS containing salts, urea, glucose, lipids, and mucin. Level 3 biorelevant media represented complete ATS containing salts, urea, glucose, lipids, mucin and proteins (albumin, lysozyme, lactoferrin and immunoglobulin G).

The volume of an eye drop ranges between approximately 25 μL and 70 μL, depending on the dispenser type, formulation physico-chemical properties and the manner in which the patient dispenses the drops (van Santvliet & Ludwig, 2004). However, the maximum fluid volume

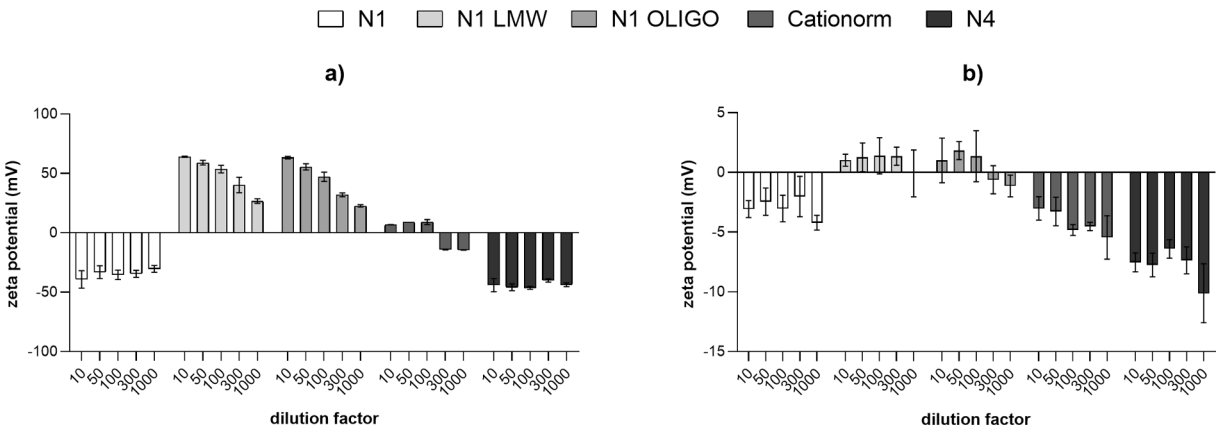

Fig. 4. Zeta potential of serially diluted NEs determined by ELS. 2.5 % glycerol (or 1.6 % glycerol in the case of Cationorm®) (a) and ATS 0 (b) were used as dilution media. Data are expressed as the mean ± SD (n = 3).

that the palpebral fissure can hold without overflowing is estimated to be 30 μL under normal conditions, when the patient is upright and not blinking. Thus, any excess eye drop volume is squeezed out of the *cul-de-sac* by blinking or drained through the nasolacrimal duct system soon after application. It is unlikely that the entire volume of an eye drop is homogenously mixed with a small TF volume (7 μL) and distributed in the form of a very thin layer over the ocular surface before elimination of its excess occurs. Therefore, for the prediction of NE stability under simulated tear turnover, the lower eye drop volume limit (25 μL) appears to be a more biorelevant choice than the mean eye drop volume of approximately 50 μL.

After mixing with tear fluid, the instilled formulation was continuously diluted and cleared from the eye surface due to tear turnover. The tear turnover rate has been estimated to be 16 ± 5 % min^{-1} (Kuppens et al., 1992, 1995; Pepić et al., 2014; van Best et al., 1995; Willcox et al., 2017).

In this study, stable and potentially less stable NEs were subjected to a biorelevant dilution simulating tear turnover with ATS of different

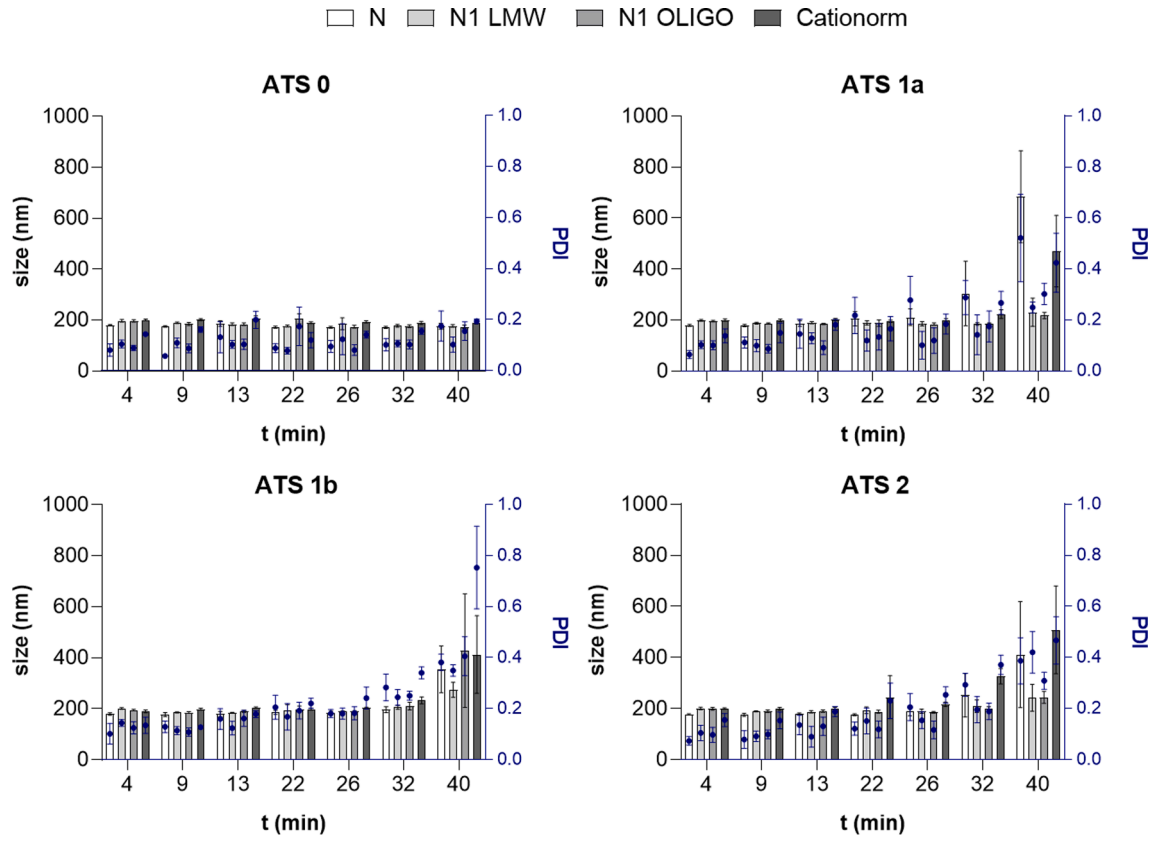

Fig. 5. Average hydrodynamic droplet size (bars) and polydispersity index (PDI, circles) of NE formulations in biorelevant conditions simulating the effect of tear turnover. The complexity level of biorelevant media, namely, artificial tear solution (ATS), differed according to the components present in the medium. Level 0 biorelevant medium contains salts, glucose, and urea (annotated as **ATS 0**). Level 1a biorelevant medium, in addition to salts, urea and glucose, contains naturally present lipids (triolein, cholesterol, oleic acid, oleic acid methyl ester, cholesteryl oleate and phosphatidylcholine) (annotated as **ATS 1a**), while level 1b biorelevant medium contains mucin (annotated as **ATS 1b**). Level 2 biorelevant medium represents complex ATS containing salts, urea, glucose, lipids, and mucin (annotated as **ATS 2**). Data are expressed as the mean ± SD (n = 3).

levels of complexity (Fig. 1). NEs were mixed with ATS in a volume ratio of 25:7, and tear turnover (16 % min^{-1}, 34 °C and 50 rpm) was simulated over a time period of 40 min. Average droplet size and PDI were determined in the 4th, 9th, 13th, 22nd, 26th, 32nd and 40th min, which corresponds to NE dilutions of approximately 2, 5, 10, 50, 100, 300 and 1000 times.

Fig. 5 shows that simulated tear turnover, in the case of the NEs diluted with ATS 0, did not cause significant changes in NE droplet size and PDI. In addition to continuous dilution, there are two additional factors that may influence the NE physical stability, namely, the incubation time and temperature (34 °C). Neither of these factors seemed to affect NE stability. However, when lipids were introduced into the ATS, the obtained results were somewhat different. The average droplet size in the NE formulation N1 and Cationorm® increased at later time points, which was accompanied by an increase in PDI. The chitosan-containing NE formulations N1 LMW and N1 OLIGO did not show a significant droplet size increase during the 40-min time period, but an increase in PDI was observed in the last investigated time point. Very similar results were obtained with the complex ATS 2, while in ATS 1b, which contained mucin but no lipids, a gradual PDI increase in all the formulations was observed, but the average droplet size increased only in the last investigated time point, and it was the least pronounced in the case of the NE formulation N1 LMW. Based on these experiments, the conclusion can be drawn that the tested NE formulations remained stable during the simulation of tear turnover *in vitro,* and the beginning of NE destabilization was detected only in the last time point of the experiment.

The stability of the potentially less stable NEs (N2, N2 LMW, N2 OLIGO, N3, and N4) under simulated tear turnover is shown in Fig. 6. The potentially less stable NE formulations were prepared with modification of the primary composition of the NEs previously confirmed to be physically stable (Jurišić Dukovski et al., 2020). The NE formulations N2, N2 LMW and N2 OLIGO with double the amount of the oil phase remained stable in all the tested dilution media. A minor increase in the average droplet size was noticed in the last investigated time point in the case of NEs diluted with ATS 1a and 2, which contained lipids. Additionally, an increase in PDI was detected, which was the most obvious in ATS 1b and ATS 2. The NE formulation N3 with half the amount of Kolliphor® EL showed similar behavior to NE formulations N2, N2 LMW and N2 OLIGO. In contrast, the NE formulation N4 without Kolliphor® EL was characterized by a major increase in average droplet size and PDI in all the biorelevant media tested. It is important to note that the increase was lower when the formulation was diluted with ATS 0 (Fig. 2), indicating that incubation time, temperature and lipids and mucin had a significant impact on NE stability.

Since both stable and potentially less stable NEs showed robustness to biorelevant dilution simulating the effect of tear turnover, testing in the most complex biorelevant medium (ATS 3) continued only with stable NE formulations and formulation N4 as a control (Fig. 1). ATS 3 was composed of salts, urea, glucose, lipids, mucin and proteins naturally present in the TF.

The results are shown in Fig. 7. The onset of an increase in average droplet size and PDI occurred earlier than in ATS 2 for all the tested formulations, which was especially pronounced in the case of the NE formulation N1. It appears that the proteins (albumin, lysozyme, lactoferrin and immunoglobulin G) present in the TF have an important impact on NE stability after application on the ocular surface. Some proteins and glycoproteins from the mucoaqueous TF layer, such as lysozyme and mucin, are thought to intercalate with the lipid layer. Additionally, it has been suggested that lipid-protein interactions play an important role in the shear thinning properties of tears (Willcox et al., 2017). The *in vitro*, *in vivo* and *in silico* evidence suggest that in the case of Cationorm®, the increase in the thickness of lipid layer of TF is a consequence of mixing of the oil phase (mineral oil) with lipid layer,

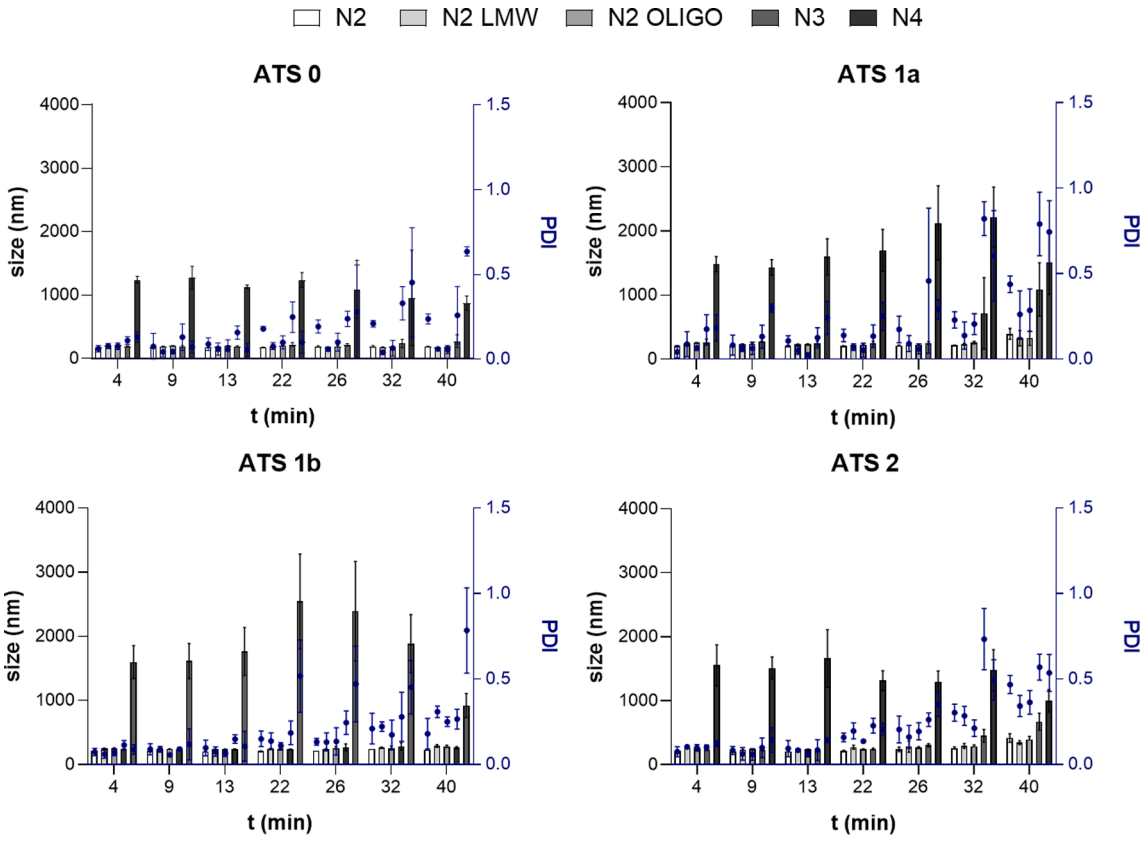

Fig. 6. Average droplet size (hydrodynamic diameter, bars) and polydispersity index (PDI, circles) of potentially less stable NE formulations in biorelevant conditions simulating the effect of tear turnover. Data are expressed as the mean ± SD (n = 2).

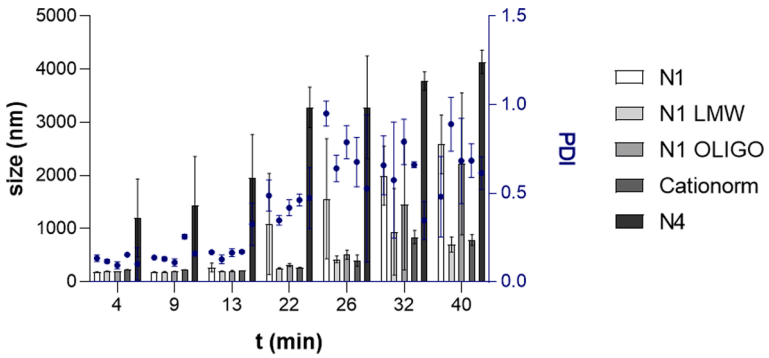

Fig. 7. Average droplet size (hydrodynamic diameter, bars) and polydispersity index (PDI, circles) of NEs in biorelevant conditions simulating the effect of tear turnover with complete artificial tear solution (**ATS 3**). Data are expressed as the mean ± SD (n = 2).

while the surface active substances (cetalkonium chloride, tyloxapol and poloxamer 188) adsorb at the lipid-mucoaqueous interface, reducing the surface tension of TF and improving the overall TF stability (Daull et al., 2020). It can be assumed that droplet breakdown precedes mixing with the TF components and that it happens soon after instillation. However, in this study, the droplets of Cationorm® and other adequately stabilized NEs (namely, NE formulations N1, N1 LMW and N1 OLIGO) began to increase in size no earlier than 22 min after the introduction of simulated tear turnover conditions in the most complex ATS 3 (Fig. 7), still rendering the droplet form.

It also appears that chitosan acts as an additional NE stabilizer, as it significantly slowed droplet growth in the diluted NEs. The mechanism behind this slowing may be the formation of an impermeable chitosan coating on the droplet surface, preventing the phenomenon of Ostwald ripening (Chiappisi & Gradzielski, 2015). The choice of chitosan type for NE preparation also appears crucial for stability, since the formulation stabilized with LM_W chitosan showed a slower droplet size increase in the biorelevant medium compared to the NE formulation stabilized with chitosan OLIGO. LM_W chitosan might have an additional steric effect that prevents collision of the nanodroplets. This effect is probably not present or is smaller in the case of chitosan OLIGO having a much lower M_w (4–6 kDa vs 50–190 kDa for OLIGO and LM_W chitosan, respectively). NE stability evaluation by measuring average droplet size and PDI under simulated tear turnover using the most complex artificial tear solution (ATS 3) was found to be sensitive to meaningful and deliberate formulation changes and discriminative toward critical material attributes such as the stabilizer type. The degradation of chitosan *in vivo* mainly occurs by hydrolysis with lysozyme, which is present in tears (Lim et al., 2008; Ren et al., 2005). However, chitosans with high DD show low degradation with lysozyme due to the lack of consecutive *N*-acetyl-D-glucosamine units and the inability of D-glucosamine units to access the lysozyme active site (Lim et al., 2008). The chitosans used in this study had high DDs (75–85 % for LM_w and >90 % for OLIGO chitosan), and it is therefore unlikely that lysozyme present in the most complex biorelevant medium (ATS 3) at a concentration of 1.9 mg mL^{-1} had a major impact on chitosan degradation during the 40-minute simulated tear turnover experiment. Åhlén et al. investigated the disintegration of chitosan poly-(acrylic acid) nanoparticles due to hydrolysis of the chitosan chains by lysozyme by monitoring the nanoparticle size (Åhlén et al., 2018). They observed no change in particle size within the first hour of nanoparticle exposure to lysozyme at concentrations ranging between 0.07 mM and 0.3 mM, which correspond to 1 mg mL^{-1} and 3 mg mL^{-1}, respectively.

In summary, the stability testing of NEs under simulated tear turnover demonstrated resistance of adequately stabilized ophthalmic NEs to destabilization. The onset of destabilization of NEs was detected only in the last time points of the experiments, when significant dilution occurred. The complexity of the bioreleveant medium plays an important role, and the most complex artificial tear solution was found to be discriminative toward critical material attributes, such as the type of stabilizer.

3.4. Nanoemulsion stability under simulated eye blinking

Another level of complexity in studying NE physical stability was added by exposing the NEs diluted with complex ATS (ATS 2) to a series of simulated eye blinks (i.e., high shear rate interspersed by rest periods) (Destruel et al., 2020) (Fig. 1). Based on the eyelid velocity and values of the TF thickness, the maximum shear rate exerted by the eyelid on the TF and instilled formulation ranges from 10^3 to 10^4 s^{-1} (Xu et al., 2015). In this study, NEs were diluted with complex ATS (ATS 2) and exposed to 10 consecutive simulated blinks. The blinks were simulated by the high shear rate of 5000 s^{-1} lasting 1 s, while the rest period between two consecutive blinks was simulated by a nondestructive oscillatory measurement at a frequency of 1 Hz and an amplitude of 1 % for 1 min. The experimental setup for assessing NE stability under simulated blinking aimed to cover the critical period for drug absorption, i.e., the period prior to excessive dilution of instilled formulation. Namely, in 10 min upon instillation (corresponding to the timeframe of the conducted simulated blinking experiment), the formulation was diluted 5 times.

The average droplet size and PDI of the NEs after 10 simulated blinks and rest periods are shown in Fig. 8. The average droplet size of the NE formulations N1, N1 LMW, N1 OLIGO and Cationorm® was unchanged throughout 10 simulated blinks, and the PDI values were 0.2 or lower, indicating monodisperse systems (Singh et al., 2017). However, the average droplet size of the NE formulation N4 with lecithin as the only surfactant changed significantly after exposure to simulated blinking. The increase in the droplet size was still smaller than the increase observed after the same dilution (9^{th} minute) in simulated tear turnover conditions in ATS 2. In the case of the NE formulation N4, factors such as dilution media and time had greater influence on the formulation stability than the force produced by blinking. Additionally, it seems that the force produced by blinking does not have any impact on the stability of adequately stabilized NE formulations N1, N1 LMW, N1 OLIGO and Cationorm®.

3.5. Limitations, challenges and future development

This study describes the development of a biorelevant *in vitro* method with the potential to predict NE stability in the TF after application. By utilizing stepwise increases in the complexity of the dilution medium, we approached realistic *in vivo* conditions and thus determined the key factors affecting NE behavior. The methods described represent an *in vitro* simulation of NE fate after application on the surface of an eye and, as such, have their own limitations. First, TF has a layered structure in which the lipid layer, as the outermost layer, covers the muco-aqueous gel adjacent to the glycocalyx and corneal and conjunctival epithelial cells (Willcox et al., 2017). On the other hand, the lipids in our study

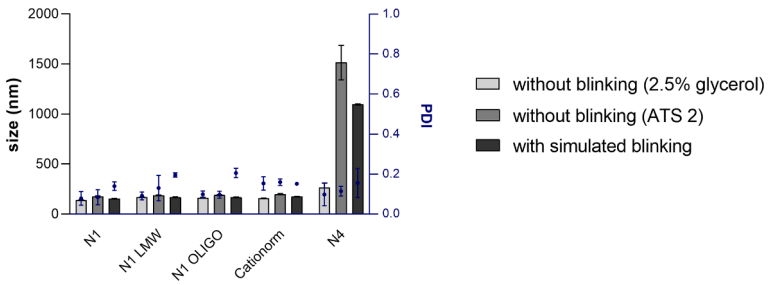

Fig. 8. Droplet size distribution (average droplet size (hydrodynamic diameter, bars) and polydispersity index (PDI, circles) of formulations in biorelevant conditions simulating the effect of eye blinking. Data are expressed as the mean ± SD (n = 3).

were homogeneously distributed in the ATS, which is different than the *in vivo* conditions. Such a difference in the organization of lipids probably leads to a different interaction pattern with the NE oily droplets, causing the deviation from the *in vivo* findings. Second, in this study, it was assumed that all the components present in the TF have the same turnover rate of 16 % min^{-1}. However, the lipid layer of TF has a much slower turnover rate (approximately 0.93 % min^{-1}) than the aqueous phase (Mochizuki et al., 2009), leading to a much longer residence of NE oil droplets/oil phase components on the eye surface. TF has a complex structure with intricate dynamics and physiology, and it is therefore not easy to mimic it *in vitro*. Moreover, a DED TF is not simply a more concentrated healthy TF, but it is characterized by changes in the concentration of TF components (e.g., salts, metabolites, lipids, proteins and mucins), some of which are more and some less or equally concentrated as in a normal, healthy TF (Willcox et al., 2017). These concentrations differ depending on the stage of DED, and their clinical significance still needs to be determined. Therefore, the composition of biorelevant ATS mimicking different stages of DED should be tailored carefully to include the key changes that could affect NE behavior in tears. Nevertheless, the proposed simple approach revealed the potential to detect differences in NE response to biorelevant stress conditions, which may be significant in NE innovative and generic formulation development.

4. Conclusions

Herein, NEs differing in critical material attributes and critical formulation variables were employed with the aim of developing a biorelevant *in vitro* method for evaluating NE stability after instillation to the eye surface. The impact of biorelevant media complexity, temperature, time and shear force produced by blinking were evaluated. According to our findings, the most discriminative method mimicking tear turnover *in vivo* was the one using the most complex biorelevant media (ATS 3).

The biorelevant *in vitro* tools simulating tear turnover and blinking will enable reliable, cost- and time-effective processes for the development of innovative nanotechnology-based topical ophthalmic formulations (e.g., NEs, liposomes, nanosuspensions, micelles, solid lipid nanoparticles, nanostructured lipid carriers), as well as more efficient development processes for complex generic ophthalmic drug products. Implementation of these tools would enable monitoring of particle/droplet properties (i.e., assessing dispersed phase stability) and/or formulation rheological behavior (i.e., predicting retention at the eye surface) when subjected to biorelevant stress conditions.

CRediT authorship contribution statement

Bisera Jurišić Dukovski: Conceptualization, Methodology, Validation, Formal analysis, Investigation, Data curation, Writing – original draft, Writing – review & editing. **Josip Ljubica:** Methodology, Validation, Formal analysis, Investigation, Data curation, Writing – original draft, Writing – review & editing. **Petra Kocbek:** Methodology, Validation, Formal analysis, Investigation, Writing – original draft, Writing – review & editing. **Maša Safundžić Kučuk:** Formal analysis, Writing – original draft, Writing – review & editing. **Iva Krtalić:** Validation, Formal analysis, Investigation, Writing – original draft, Writing – review & editing. **Anita Hafner:** Formal analysis, Investigation, Writing – original draft, Writing – review & editing. **Ivan Pepić:** Formal analysis, Investigation, Writing – original draft, Writing – review & editing. **Jasmina Lovrić:** Conceptualization, Methodology, Validation, Formal analysis, Investigation, Resources, Writing – original draft, Writing – review & editing, Supervision, Project administration, Funding acquisition.

Declaration of Competing Interest

The authors declare that they have no known competing financial interests or personal relationships that could have appeared to influence the work reported in this paper.

Data availability

Data will be made available on request.

Acknowledgments

This work was supported by the project BeatDED (IP-2019-04-2174) funded by the Croatian Science Foundation and project FarmInova (KK.01.1.1.02.0021) funded by the European Regional Development Fund. Josip Ljubica is the recipient of a PhD fellowship funded by the European Social Fund under the Croatian Science Foundation project (programme Young researchers' career development project – training of new doctoral students, DOK-2020-01-4932). The graphical abstract was created with BioRender.com.

References

Abelson, M.B., Udell, I.J., Weston, J.H., 1981. Normal human tear pH by direct measurement. Arch. Ophthalmol. 99 (2) https://doi.org/10.1001/archopht.1981.03930010303017.

Åhlén, M., Tummala, G.K., Mihranyan, A., 2018. Nanoparticle-loaded hydrogels as a pathway for enzyme-triggered drug release in ophthalmic applications. Int. J. Pharm. 536 (1) https://doi.org/10.1016/j.ijpharm.2017.11.053.

Bellantone, R.A., Shah, K.B., Patel, P.G., Kaplan, M., Xu, X., Li, V., Newman, B., Abul Kaisar, M., 2022. Cyclosporine release and distribution in ophthalmic emulsions determined by pulsatile microdialysis. Int. J. Pharm. 615 https://doi.org/10.1016/j.ijpharm.2022.121521.

Chiappisi, L., & Gradzielski, M. (2015). Co-assembly in chitosan-surfactant mixtures: Thermodynamics, structures, interfacial properties and applications. In *Advances in Colloid and Interface Science* (Vol. 220). https://doi.org/10.1016/j.cis.2015.03.003.

Daull, P., Amrane, M., Ismail, D., Georgiev, G., Cwiklik, L., Baudouin, C., Leonardi, A., Garhofer, G., Garrigue, J.S., 2020. Cationic Emulsion-Based Artificial Tears as a Mimic of Functional Healthy Tear Film for Restoration of Ocular Surface Homeostasis in Dry Eye Disease. J. Ocul. Pharmacol. Ther. 36 (6) https://doi.org/10.1089/jop.2020.0011.

Dean, A.W., Glasgow, B.J., 2012. Mass spectrometric identification of phospholipids in human tears and tear lipocalin. Invest. Ophthalmol. Vis. Sci. 53 (4) https://doi.org/10.1167/iovs.11-9419.

Destruel, P.L., Zeng, N., Seguin, J., Douat, S., Rosa, F., Brignole-Baudouin, F., Dufaÿ, S., Dufaÿ-Wojcicki, A., Maury, M., Mignet, N., Boudy, V., 2020. Novel in situ gelling ophthalmic drug delivery system based on gellan gum and hydroxyethylcellulose:

Innovative rheological characterization, in vitro and in vivo evidence of a sustained precorneal retention time. Int. J. Pharm. 574 https://doi.org/10.1016/j.ijpharm.2019.118734.

Gan, L., Wang, J., Jiang, M., Bartlett, H., Ouyang, D., Eperjesi, F., Liu, J., & Gan, Y. (2013). Recent advances in topical ophthalmic drug delivery with lipid-based nanocarriers. In *Drug Discovery Today* (Vol. 18, Issues 5–6). https://doi.org/10.1016/j.drudis.2012.10.005.

Georgiev, G.A., Yokoi, N., Nencheva, Y., Peev, N., Daull, P., 2017. Surface chemistry interactions of cationorm with films by human meibum and tear film compounds. Int. J. Mol. Sci. 18 (7) https://doi.org/10.3390/ijms18071558.

Isailović, T., Đorđević, S., Marković, B., Randelovic, D., Cekić, N., Lukić, M., Pantelić, I., Daniels, R., Savić, S., 2016. Biocompatible Nanoemulsions for Improved Aceclofenac Skin Delivery: Formulation Approach Using Combined Mixture-Process Experimental Design. J. Pharm. Sci. 105 (1) https://doi.org/10.1002/jps.24706.

Israelachvili, J., 2011. Intermolecular and Surface Forces. In *Intermolecular and Surface Forces*. https://doi.org/10.1016/C2009-0-21560-1.

Jones, L., Downie, L.E., Korb, D., Benitez-del-Castillo, J.M., Dana, R., Deng, S.X., Dong, P. N., Geerling, G., Hida, R.Y., Liu, Y., Seo, K.Y., Tauber, J., Wakamatsu, T.H., Xu, J., Wolffsohn, J.S., Craig, J.P., 2017. TFOS DEWS II Management and Therapy Report. In *Ocular Surface* Vol. 15, Issue 3. https://doi.org/10.1016/j.jtos.2017.05.006.

Jurišić Dukovski, B., Juretić, M., Bračko, D., Randjelović, D., Savić, S., Crespo Moral, M., Diebold, Y., Filipović-Grčić, J., Pepić, I., Lovrić, J., 2020. Functional ibuprofen-loaded cationic nanoemulsion: Development and optimization for dry eye disease treatment. Int. J. Pharm. 576 https://doi.org/10.1016/j.ijpharm.2019.118979.

Kaszuba, M., Corbett, J., Watson, F.M.N., Jones, A., 2010. High-concentration zeta potential measurements using light-scattering techniques. Philos. Trans. R. Soc. A Math. Phys. Eng. Sci. 368 (1927) https://doi.org/10.1098/rsta.2010.0175.

Khatri, P., Shao, J., 2017. Separation of external aqueous phase from o/w nanoemulsions. Eur. J. Pharm. Sci. 96 https://doi.org/10.1016/j.ejps.2016.09.021.

Krämer, W., Grapentin, C., Bouvain, P., Temme, S., Flögel, U., Schubert, R., 2019. Rational manufacturing of functionalized, long-term stable perfluorocarbon-nanoemulsions for site-specific 19F magnetic resonance imaging. Eur. J. Pharm. Biopharm. 142 https://doi.org/10.1016/j.ejpb.2019.06.014.

Kumar, N., Mandal, A., 2018. Thermodynamic and physicochemical properties evaluation for formation and characterization of oil-in-water nanoemulsion. J. Mol. Liq. 266 https://doi.org/10.1016/j.molliq.2018.06.069.

Kuppens, E.V.M.J., Stolwijk, T.R., de Keizer, R.J.W., van Best, J.A., 1992. Basal tear turnover and topical timolol in glaucoma patients and healthy controls by fluorophotometry. Invest. Ophthalmol. Vis. Sci. 33 (12).

Kuppens, E.V.M.J., van Best, J.A., Sterk, C.C., de Keizer, R.J.W., 1995. Decreased basal tear turnover in patients with untreated primary open- angle glaucoma. Am. J. Ophthalmol. 120 (1) https://doi.org/10.1016/S0002-9394(14)73757-2.

Lallemand, F., Daull, P., Benita, S., Buggage, R., Garrigue, J.-S., 2012. Successfully Improving Ocular Drug Delivery Using the Cationic Nanoemulsion. Novasorb. *Journal of Drug Delivery* 2012. https://doi.org/10.1155/2012/604204.

Lefebvre, G., Riou, J., Bastiat, G., Roger, E., Frombach, K., Gimel, J.C., Saulnier, P., Calvignac, B., 2017. Spontaneous nano-emulsification: Process optimization and modeling for the prediction of the nanoemulsion's size and polydispersity. Int. J. Pharm. 534 (1–2) https://doi.org/10.1016/j.ijpharm.2017.10.017.

Lim, S.M., Song, D.K., Oh, S.H., Lee-Yoon, D.S., Bae, E.H., Lee, J.H., 2008. In vitro and in vivo degradation behavior of acetylated chitosan porous beads. J. Biomater. Sci. Polym. Ed. 19 (4) https://doi.org/10.1163/156856208783719482.

Lorentz, H., Heynen, M., Kay, L.M.M., Dominici, C.Y., Khan, W., Ng, W.W.S., Jones, L., 2011. Contact lens physical properties and lipid deposition in a novel characterized artificial tear solution. Mol. Vis. 17.

Maïssa, C., Guillon, M., Simmons, P., Vehige, J., 2010. Effect of castor oil emulsion eyedrops on tear film composition and stability. Cont. Lens Anterior Eye 33 (2). https://doi.org/10.1016/j.clae.2009.10.005.

McClements, D.J., 2015. Gastrointestinal Fate of Emulsions. In *Food Emulsions*. https://doi.org/10.1201/b18868-13.

Mochizuki, H., Yamada, M., Hatou, S., Tsubota, K., 2009. Turnover rate of tear-film lipid layer determined by fluorophotometry. Br. J. Ophthalmol. 93 (11) https://doi.org/10.1136/bjo.2008.156828.

Ozturk, B., Argin, S., Ozilgen, M., McClements, D.J., 2014. Formation and stabilization of nanoemulsion-based vitamin e delivery systems using natural surfactants: Quillaja saponin and lecithin. J. Food Eng. 142 https://doi.org/10.1016/j.jfoodeng.2014.06.015.

Pepić, I., Lovrić, J., Cetina-Čižmek, B., Reichl, S., Filipović-Grčić, J., 2014. Toward the practical implementation of eye-related bioavailability prediction models. Drug Discov. Today 19 (1), 31–44. https://doi.org/10.1016/j.drudis.2013.08.002.

Petrochenko, P.E., Pavurala, N., Wu, Y., Yee Wong, S., Parhiz, H., Chen, K., Patil, S.M., Qu, H., Buoniconti, P., Muhammad, A., Choi, S., Kozak, D., Ashraf, M., Cruz, C.N., Zheng, J., Xu, X., 2018. Analytical considerations for measuring the globule size distribution of cyclosporine ophthalmic emulsions. Int. J. Pharm. 550 (1–2) https://doi.org/10.1016/j.ijpharm.2018.08.030.

Ragheb, R., Nobbmann, U., 2020. Multiple scattering effects on intercept, size, polydispersity index, and intensity for parallel (VV) and perpendicular (VH) polarization detection in photon correlation spectroscopy. Sci. Rep. 10 (1) https://doi.org/10.1038/s41598-020-78872-4.

Ren, D., Yi, H., Wang, W., Ma, X., 2005. The enzymatic degradation and swelling properties of chitosan matrices with different degrees of N-acetylation. Carbohydr. Res. 340 (15) https://doi.org/10.1016/j.carres.2005.07.022.

Sandoval-Cuellar, C.E., de Jesus Perea-Flores, M., Quintanilla-Carvajal, M.X., 2020. In-vitro digestion of whey protein- and soy lecithin-stabilized High Oleic Palm Oil emulsions. J. Food Eng. 278 https://doi.org/10.1016/j.jfoodeng.2020.109918.

Savić, V., Ilić, T., Nikolić, I., Marković, B., Čalija, B., Cekić, N., Savić, S., 2019. Tacrolimus-loaded lecithin-based nanostructured lipid carrier and nanoemulsion with propylene glycol monocaprylate as a liquid lipid: Formulation characterization and assessment of dermal delivery compared to referent ointment. Int. J. Pharm. 569 https://doi.org/10.1016/j.ijpharm.2019.118624.

Saville, J.T., Zhao, Z., Willcox, M.D.P., Ariyavidana, M.A., Blanksby, S.J., Mitchell, T.W., 2011. Identification of phospholipids in human meibum by nano-electrospray ionisation tandem mass spectrometry. Exp. Eye Res. 92 (3) https://doi.org/10.1016/j.exer.2010.12.012.

Singh, M., Bharadwaj, S., Lee, K.E., Kang, S.G., 2020. Therapeutic nanoemulsions in ophthalmic drug administration: Concept in formulations and characterization techniques for ocular drug delivery. In. J. Control. Release 328. https://doi.org/10.1016/j.jconrel.2020.10.025.

Singh, Y., Meher, J.G., Raval, K., Khan, F.A., Chaurasia, M., Jain, N.K., Chourasia, M.K., 2017. Nanoemulsion: Concepts, development and applications in drug delivery. In. J. Control. Release 252. https://doi.org/10.1016/j.jconrel.2017.03.008.

Stevenson, D., Tauber, J., Reis, B.L., 2000. Efficacy and safety of cyclosporin A ophthalmic emulsion in the treatment of moderate-to-servere dry eye disease: A dose-ranging, randomized trial. Ophthalmology 107 (5). https://doi.org/10.1016/S0161-6420(00)00035-X.

Tadros, T., Izquierdo, P., Esquena, J., Solans, C., 2004. Formation and stability of nano-emulsions. Adv. Colloid Interface Sci. 108–109 https://doi.org/10.1016/j.cis.2003.10.023.

van Best, J.A., del Castillo Benitez, J.M., Coulangeon, L.M., 1995. Measurement of basal tear turnover using a standardized protocol - European Concerted Action on Ocular Fluorometry. *Graefe's Archive for*. Clin. Experiment. Ophthalmol. 233 (1) https://doi.org/10.1007/BF00177778.

van Santvliet, L., & Ludwig, A. (2004). Determinants of eye drop size. In *Survey of Ophthalmology* (Vol. 49, Issue 2). https://doi.org/10.1016/j.survophthal.2003.12.009.

Walenga, R.L., Babiskin, A.H., Zhang, X., Absar, M., Zhao, L., Lionberger, R.A., 2019. Impact of Vehicle Physicochemical Properties on Modeling-Based Predictions of Cyclosporine Ophthalmic Emulsion Bioavailability and Tear Film Breakup Time. J. Pharm. Sci. 108 (1) https://doi.org/10.1016/j.xphs.2018.10.034.

Willcox, M.D.P., Argüeso, P., Georgiev, G.A., Holopainen, J.M., Laurie, G.W., Millar, T.J., Papas, E.B., Rolland, J.P., Schmidt, T.A., Stahl, U., Suarez, T., Subbaraman, L.N., Uçakhan, O., Jones, L., 2017. TFOS DEWS II Tear Film Report. In *Ocular Surface* Vol. 15, Issue 3. https://doi.org/10.1016/j.jtos.2017.03.006.

Xu, X., Al-Ghabeish, M., Rahman, Z., Krishnaiah, Y.S.R., Yerlikaya, F., Yang, Y., Manda, P., Hunt, R.L., Khan, M.A., 2015. Formulation and process factors influencing product quality and in vitro performance of ophthalmic ointments. Int. J. Pharm. 493 (1–2) https://doi.org/10.1016/j.ijpharm.2015.07.066.